Accepted Manuscript

The chemosensitizing agent lubeluzole binds calmodulin and inhibits Ca^{2+}/calmodulin-dependent kinase II

Claudio Bruno, Dr. Maria Maddalena Cavalluzzi, Ph. D, Maria Rosaria Rusciano, Angelo Lovece, Antonio Carrieri, Riccardo Pracella, Giulia Giannuzzi, Lorenzo Polimeno, Maurizio Viale, Maddalena Illario, Carlo Franchini, Giovanni Lentini

PII: S0223-5234(16)30227-6

DOI: 10.1016/j.ejmech.2016.03.045

Reference: EJMECH 8470

To appear in: *European Journal of Medicinal Chemistry*

Received Date: 10 July 2015

Revised Date: 16 March 2016

Accepted Date: 17 March 2016

Please cite this article as: C. Bruno, M.M. Cavalluzzi, M.R. Rusciano, A. Lovece, A. Carrieri, R. Pracella, G. Giannuzzi, L. Polimeno, M. Viale, M. Illario, C. Franchini, G. Lentini, The chemosensitizing agent lubeluzole binds calmodulin and inhibits Ca^{2+}/calmodulin-dependent kinase II, *European Journal of Medicinal Chemistry* (2016), doi: 10.1016/j.ejmech.2016.03.045.

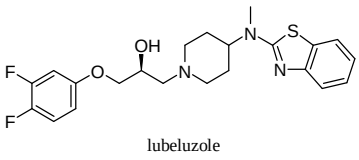

lubeluzole

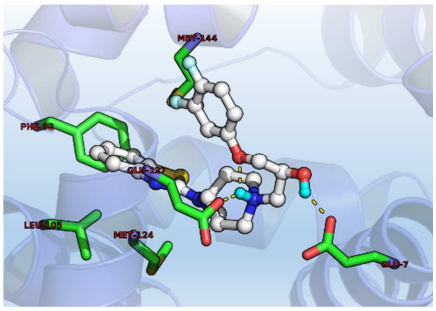

The chemosensitizing agent lubeluzole binds calmodulin and inhibits Ca^{2+}/calmodulin-dependent kinase II

Claudio Bruno,[a] Maria Maddalena Cavalluzzi,[a*] Maria Rosaria Rusciano,[b] Angelo Lovece,[a] Antonio Carrieri,[a] Riccardo Pracella,[a] Giulia Giannuzzi,[c] Lorenzo Polimeno,[d] Maurizio Viale,[e] Maddalena Illario,[b] Carlo Franchini,[a] Giovanni Lentini.[a]

[a]*Dipartimento di Farmacia – Scienze del Farmaco, Università degli Studi di Bari 'Aldo Moro', via E. Orabona 4, 70126 Bari, Italy.*

[b]*Dipartimento di Biologia e Patologia Cellulare e Molecolare, Università Federico II, 80131 Napoli, Italy.*

[c] *Dipartimento di Bioscienze, Biotecnologie e Biofarmaceutica, Università degli Studi di Bari 'Aldo Moro', via E. Orabona 4, 70126 Bari, Italy.*

[d]*Dipartimento dell'Emergenza e dei Trapianti di Organi, Policlinico - P.zza Giulio Cesare - 70124 Bari, Italy.*

[e]*IRCCS Azienda Ospedaliera Universitaria San Martino - IST Istituto Nazionale per la Ricerca sul Cancro (IRCCS SMIST), U.O.C. Terapia Immunologia, L.go R. Benzi, 10, 16132 Genova, Italy.*

***Corresponding author:**

Dr. M. M. Cavalluzzi, Ph. D.

Dipartimento di Farmacia – Scienze del Farmaco

Università degli Studi di Bari 'Aldo Moro'

via Orabona 4, 70125 Bari, Italy

phone number: +39 080 5442232

fax number: +39 080 5442724

E-mail address: mariamaddalena.cavalluzzi@uniba.it

Abstract

An affinity capillary electrophoresis (ACE) method to estimate apparent dissociation constants between bovine brain calmodulin (CaM) and non-peptidic ligands was developed. The method was validated reproducing the dissociation constants of a number of well-known CaM ligands. In particular, the potent antagonist 125-C9 was *ad hoc* synthesized through an improved synthetic procedure. The ACE method was successfully applied to verify CaM affinity for lubeluzole, a well-known neuroprotective agent recently proved useful to potentiate the activity of anti-cancer drugs. Lubeluzole was slightly less potent than 125-C9 (K_d = 2.9 ± 0.7 and 0.47 ± 0.06 μM respectively) and displayed Ca^{2+}/calmodulin-dependent kinase II (CaMKII) inhibition (IC_{50} = 40 ± 1 μM). Possible binding modes of lubeluzole to CaM were explored by docking studies based on the X-ray crystal structures of several trifluoperazine-CaM complexes. An estimated dissociation constant in good agreement with the experimental one was found and the main aminoacidic residues and interactions contributing to complex formation were highlighted. The possibility that interference with Ca^{2+} pathways may contribute to the previously observed chemosensitizing effects of lubeluzole on human ovarian adenocarcinoma and lung carcinoma cells are discussed.

Keywords: lubeluzole, calmodulin, affinity capillary electrophoresis, anti-cancer activity, human carcinoma cells, voltage-gated sodium channels, docking.

1. Introduction

Lubeluzole [(*S*)-**1**, Fig. 1] is a homochiral benzothiazole derivative that has shown neuroprotective properties in preclinical models of ischemic stroke. Several possible mechanisms have been hypothesized to justify its beneficial activity, including inhibition of glutamate release, inhibition of glutamate-activated nitric oxide (NO) synthesis, and blockade of voltage-gated calcium channels [1–4]. Also epigenetic control on NO synthase (NOS) and calmodulin (CaM) activities has been hypothesized [2]. Recently, lubeluzole was proved to synergize with both doxorubicin and paclitaxel on human ovarian adenocarcinoma A2780 and human lung carcinoma A549 cells, respectively [5]. This activity might stem from either some of the above mechanisms or the well-known lubeluzole voltage-gated sodium channel (VGSC) blocking activity [6–8]. However, the synergistic effects of lubeluzole for both drugs were observed over a wide concentration window (0.005–5 μM), the lowest limit being at least 40 times lower than human plasma concentrations clinically relevant for the anti-ischemic activity [9] and more than 100 times lower than IC_{50} values for VGSC [6]. Thus, the possibility of concurrence of other molecular mechanisms contributing to lubeluzole chemosensitizing activity has to be hypothesized.

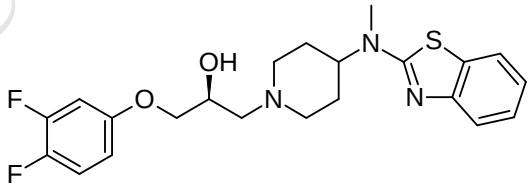

(*S*)-**1**

Fig. 1. Structure of lubeluzole.

CaM is a small ubiquitous acidic protein that acts as a Ca^{2+}-sensor and modulates the activity of several proteins [10]. Several anticancer agents bind to CaM [11], and a number of CaM ligands act as chemosensitizing agents [12–14]. Finally, several CaM ligands inhibit Ca^{2+}/CaM-dependent kinase II (CaMKII) [15] and the basic biological function of CaMKII is involved in several cancers [16–19]. This is why CaMKII inhibitors have been suggested as possible anti-cancer agents [20]. Interestingly, several known CaM ligands, such as loperamide and trifluoperazine (Fig. 2), share common structural features with lubeluzole. Therefore, we wondered if lubeluzole might interfere with Ca^{2+} pathways by binding CaM, thus potentiating the activity of anti-cancer agents. Several methodologies for the determination of dissociation constants between CaM and small molecules have been proposed. They are based on NMR [21,24], CD [22,24], fluorescence spectroscopy [23–25], gel mobility shift assays [24], enzymatic competition assays [24], chromatography on CaM-sepharose gel [26], binding assays with tritiated ligands [27,28], and isothermal titration calorimetry [15]. Most of the above methods involve the synthesis of chromophoric or radioactive ligands [25,27,28], the preparation of ^{13}C [24], ^{15}N [21], or chromophoric labeled CaM [23]. Several methods require large amounts of CaM and do not allow accurate K_d determination [22,24,26]. Finally, biochemical assays require enzymes, cofactors, and substrates [24] while isothermal titration calorimetry is quite unpractical [15].

Compared with the above reported methods, affinity capillary electrophoresis (ACE) offers some advantages in the determination of apparent dissociation constants, such as small amount of protein and ligands, and short time for each analysis. ACE does not require high purity ligands, since K_d values are based on migration times and not on peak integration. Finally, native protein in a homogeneous aqueous medium is used. Thus, the experimental setting reasonably

approximates the physiological environment of the protein and reliable affinity measures can be obtained. Here we report an ACE method to estimate apparent dissociation constants between CaM and non-peptidic, protonatable compounds. Since most of the available CaM ligands are old molecules displaying affinity at the micromolar level, we decided to synthesize a recently reported potent CaM antagonist, 125-C9 [15], as a reference compound, trying to improve the early reported synthetic procedure. Once proven the affinity of lubeluzole for CaM, its possible antagonist behaviour on CaMKII has been investigated and its possible binding mode has been explored by docking simulations carried out on properly selected crystallographic structures of CaM-antagonist complex.

2. Results and discussion

2.1. Ca^{2+}/CaM antagonism

Since the amino acid sequence of CaM is completely invariant (100% identity) among all vertebrates [29], we choose the relatively less expensive and widely used [11,22,43,53] bovine brain CaM to develop our ACE assay. We got inspiration from a pioneering ACE method used to measure binding constants of acidic 4-alkylbenzenesulfonamides to carbonic anhydrase B (CAB) [30]. This method measures changes in CAB electrophoretic mobility (μ^{ep}) in relation to various concentrations of charged ligands in the run buffer. The observed CAB μ^{ep} variations were caused by the changes in CAB charge (from Z to $Z \pm z$, where Z and z indicate the charges of CAB and the ligand, respectively), while the changes in CAB μ^{ep} caused by the changes in mass were relatively small. However, the original framework was modified in order to make CaM affinity assay reliability as high as possible. Most of the values reported in the literature for CaM ligands are derived running experiments at pH 7.4, under the assumption that the latter may be

assumed as 'the physiological pH'. Indeed, this statement holds for circulating and interstitial fluids. However, when drugs supposed to operate in intracellular environments of solid tumors are concerned, further aspects should be taken into account. First of all, intracellular pH (pH_i) may present deviations from neutrality, generally being more alkaline (>7.6) than that of normal cells [31,32]. Furthermore, the relative permittivity (ε_r) of the aqueous medium lowers at the protein surface [33]. Thus, protonatable CaM ligands should experiment microenvironmental conditions unfavorable for protonation. Indeed, CaM antagonists widely protonated at pH 7.4 (e.g. trifluoperazine and W-7, Fig. 2) form only few, non-specific ionic interactions with CaM [34], with the binding being mainly driven by the hydrophobic effect [35]. The above considerations suggested the adoption of a relatively alkaline operational pH [8,35] roughly centered on pK_as range of the known CaM ligands used as the training set (Fig. 2 and Table S1). Unfortunately, at these pH values the shift in CaM μ^{ep} caused by the interaction of the selected set of compounds (Table S1) with CaM was expected to be negligible. In fact, at pH 8.35 the migration time of CaM, injected as a sample, was not influenced by the presence of various concentrations of the ligands in the buffer. This is why we employed a reversed procedure in which buffers containing different concentrations of CaM were used to evaluate the changes of migration times of each ligand injected as a sample. A saturating concentration of $CaCl_2$ was used to activate CaM through the formation of Ca^{2+}-CaM complex in conditions previously reported as granting physiological Ca^{2+}-binding properties of CaM [36]. Glycine/tris buffer was preferred to borate buffer because the latter causes current decrease in the presence of $CaCl_2$ (chelating conditions) [37]. In order to minimize the use of the relatively costly protein, the partial filling technique, i.e. partial-filling ACE (PFACE), was used. Here, zones of protein are used in place of the column being completely filled with the analyte, thereby reducing the

amounts of sample required for the binding assay. In particular, we used flow-through partial-filling affinity capillary electrophoresis (FTPFACE) [38] to estimate the dissociation constants of well-known protonatable CaM ligands (Fig. 2) considered as a training set. While in PFACE the capillary is partially filled with a plug of ligand and receptor, and electrophoresed, in this technique we introduced a plug of CaM solubilized in the run buffer and then a smaller plug of the ligands. Thus, applying the voltage, the plug of basic samples flowed through the acidic CaM plug (Fig. S1). Scatchard analysis of the changes in ligand migration times relative to the non interacting peak of EOF, as a function of the CaM concentration, yields K_d values obtained repeating the experiments two or three times.

As an example, the superimposition of six electropherograms obtained for trifluoperazine is shown in Fig. 3A. The lower electropherogram corresponds to trifluoperazine run in the absence of CaM. The migration time of the sample was about 5 minutes. Going up, electropherograms of trifluoperazine in the presence of growing concentrations of CaM are shown. Trifluoperazine peak (indicated by an arrow) slows down with increasing concentration of CaM. Scatchard plots from a triplicate experiment are shown in Fig. 3C.

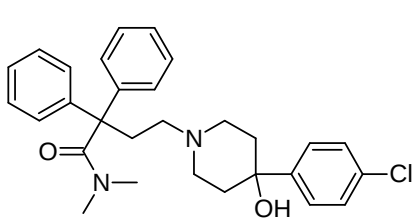

loperamide

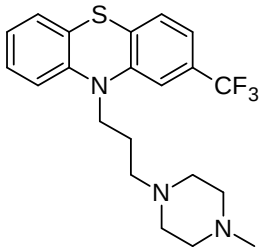

trifluoperazine

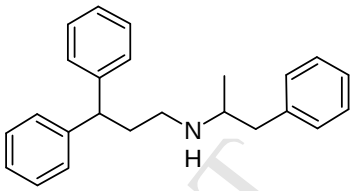

prenylamine

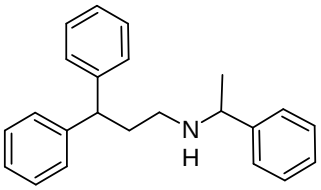

fendiline

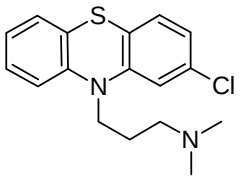

chlorpromazine

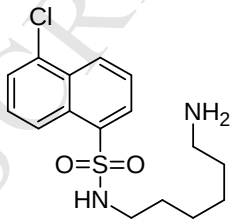

W-7

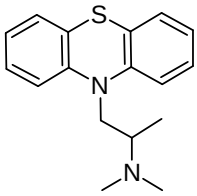

promethazine

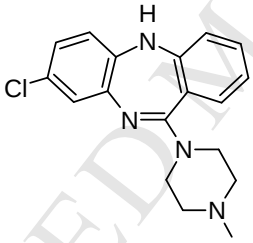

clozapine

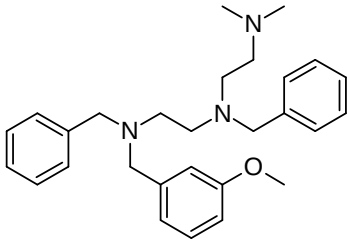

125-C9

Fig. 2. Structures of well-known protonatable CaM ligands.

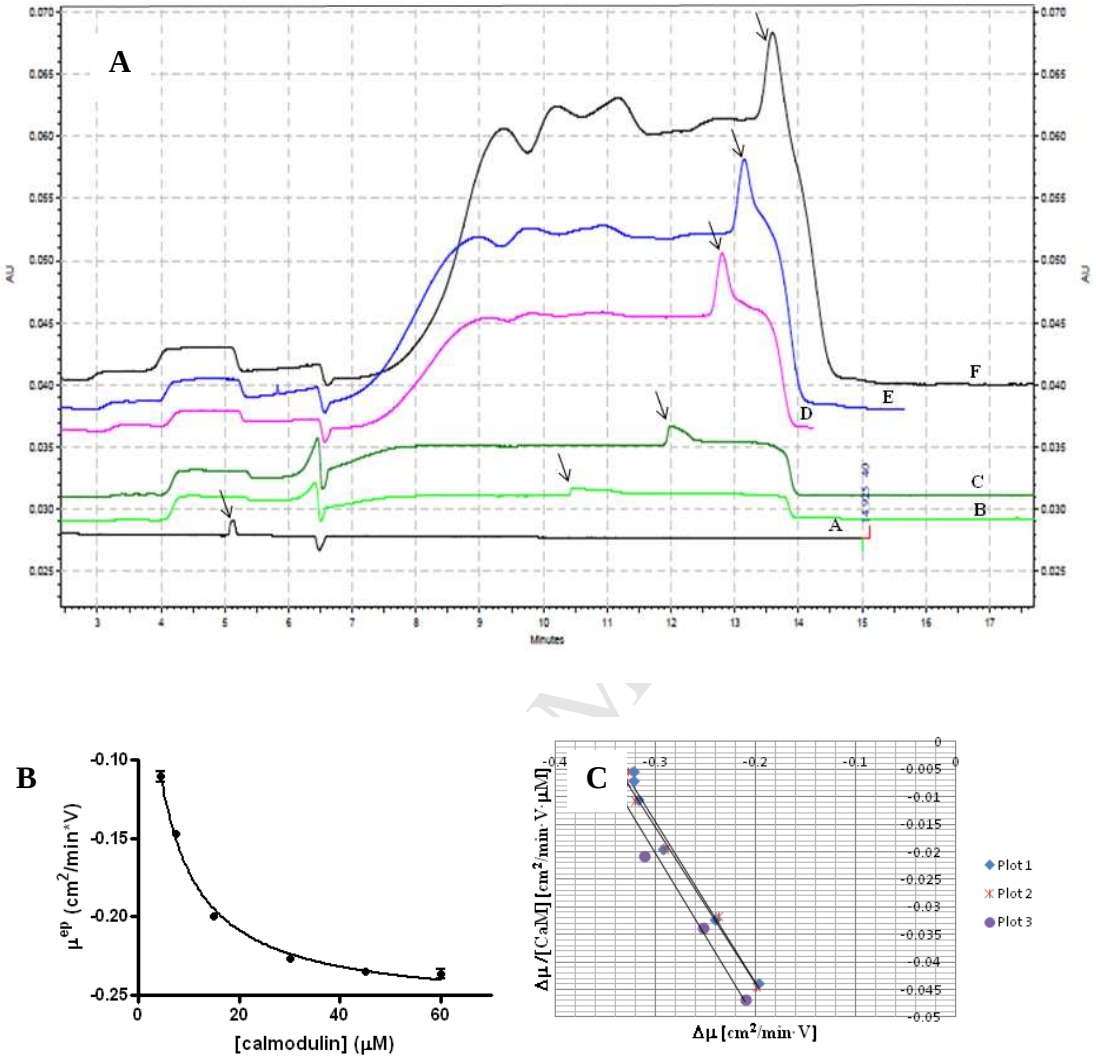

Fig. 3. A) Superimpositions of electropherograms of trifluoperazine alone (A) and in the presence of growing concentrations of CaM (B, 7.5 mM CaM; C, 15 mM CaM; D, 30 mM CaM; E, 45 mM; F, 60 mM CaM). **B)** Binding curve of trifluoperazine-CaM. **C**) Scatchard plots from triplicate experiment on trifluoperazine-CaM binding.

For the training set ligands (Fig. 2), K_d values were obtained averaging the values obtained from the Scatchard plots of at least two data sets and were in agreement with those reported in the literature (Table 1 and S2). We found that the higher the apparent K_d of the ligands (entries

6–8), the greater the standard deviation of the measurement. It is noteworthy that the method was applicable to ligands in complex mixtures: loperamide and chlorpromazine affinity values were acquired from direct analysis on their samples obtained from their corresponding pharmaceuticals.

The method was applied to verify CaM affinity for lubeluzole which displayed a K_d value of 2.9 ± 0.7 μM.

Table 1.
Comparison of apparent K_d values obtained through the FTPFACE method for selected CaM ligands and corresponding K_d, or IC_{50}, or K_i values reported in the literature.

Entry	compound	FTPFACE K_d values (μM)[a]	K_d (μM)	IC_{50} (μM)
1	trifluoperazine	3.4 ± 0.1	5[a]	–
2	prenylamine	1.80 ± 0.06	0.5–0.7[a]	–
3	fendiline	2.9 ± 0.1	0.5–0.7[a]	–
4	loperamide	3.5 ± 0.5	–	12[c]
5	chlorpromazine	3.1 ± 0.5	–	8[d]
6	promethazine	50 ± 20	–	60[d]
7	W-7	12 ± 4	7.2[a]	13.6[e]
8	clozapine	61 ± 23	–	20[d]
9	lubeluzole	2.9 ± 0.7	–	–
10	125-C9	0.47 ± 0.06	0.85[b]	–

[a] see ref 53; [b] see ref 15; [c] see ref 54; [d] see ref 55; [e] see ref 56.

The CaMKII inhibitory effect of lubeluzole was then evaluated *in vitro* following a previously reports assay [39] and, as shown in Table 2, it exerted an inhibitory activity slightly higher than that of the well-known CaMKII inhibitor W-7 and quite comparable with the novel Ca^{2+}/CaM antagonist 125-C9. Thus, it is conceivable that lubeluzole, similarly to W-7 and 125-C9, inhibits CaMKII binding competitively with CaM.

Table 2
Inhibition of CaMKII activity by W-7, 125-C9, and lubeluzole[a]

Compounds	IC_{50} ± SEM (μM)
W-7	50 ± 2[b]
125-C9	35 ± 2[c]
lubeluzole	40 ± 1

[a] CaM was used at 5 μM, values represent the mean of three independent determinations; [b] 100 μM (at 0.5 μM CaM), see ref 57; [c] 40.4 μM (at 2 μM CaM), see ref 15.

2.2. Chemistry

*2.2.1. Lubeluzole [(S)-**1**] preparation*

Lubeluzole [(*S*)-**1**] was prepared following a synthetic route based on the hydrolytic kinetic resolution reported in our previous work [5], as outlined in scheme 1. Unlike the early reported procedure, the glycidyl ether (*RS*)-**4** was synthesized following the Williamson procedure. The first attempt performed by reacting **2** with (*RS*)-**3** in NaOH solution [40] gave the desired product in acceptable yield (45%) but the parasitic formation of 1-chloro-3-(3,4-difluorophenoxy)propan-2-ol was observed too. Although the latter compound is a useful intermediate in the synthesis of lubeluzole [41], we tried to optimized the reaction conditions in order to improve (*RS*)-**4** yield. Thus, modifying a literature procedure [42], the reaction was performed in CH_3CN and in the presence of Cs_2CO_3 giving (*RS*)-**4** in 88% yield, thus improving the overall yield of lubeluzole from 30% [5] to 38%. The attempt to perform the Williamson reaction under microwave irradiation at 130 °C for 20 min failed.

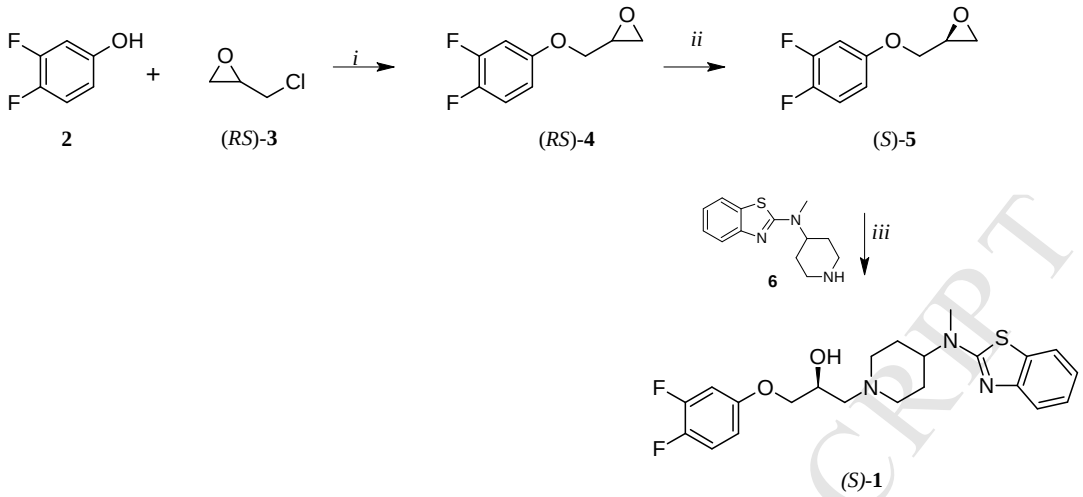

Scheme 1. *Reagents and conditions*: (i) Cs_2CO_3, MeCN, reflux; (ii) (*R*,*R*)-(salen)Co^{III}(OAc), H_2O, room temp; (iii) $Yb(OTf)_3$, anhyd CH_2Cl_2, room temp.

2.2.2. 125-C9 preparation

125-C9 was prepared by modifying a literature procedure [15] which started from the acylation of *N*,*N*'-dibenzylethylenediamine (**7**) with 3-methoxybenzoyl chloride to give *N*-benzyl-*N*-[2-(benzylamino)ethyl]-3-methoxybenzamide (**8**, scheme 2). Considering that the low yield reported in the literature for **8** (19%) was caused by the formation of **9** as a side product, we optimized the experimental conditions in order to enhance the monoacylation product yield. Thus, the reaction was performed at 0 °C for 2 h by using DBU as a base and **8** was obtained in 51% yield. Furthermore, by submitting **9** to a partial hydrolysis with 12 M HCl under microwave irradiation, the overall yield of **8** increased to 60%. In the next step, **8** was reacted with *N*,*N*-dimethylglycine under microwave irradiation, in the presence of EEDQ, and the intermediate **10** was obtained in 65% yield (versus 40% [15]). Finally, reduction of **10** gave 125-C9 (82%) which was converted into its hydrochloride salt with gaseous HCl.

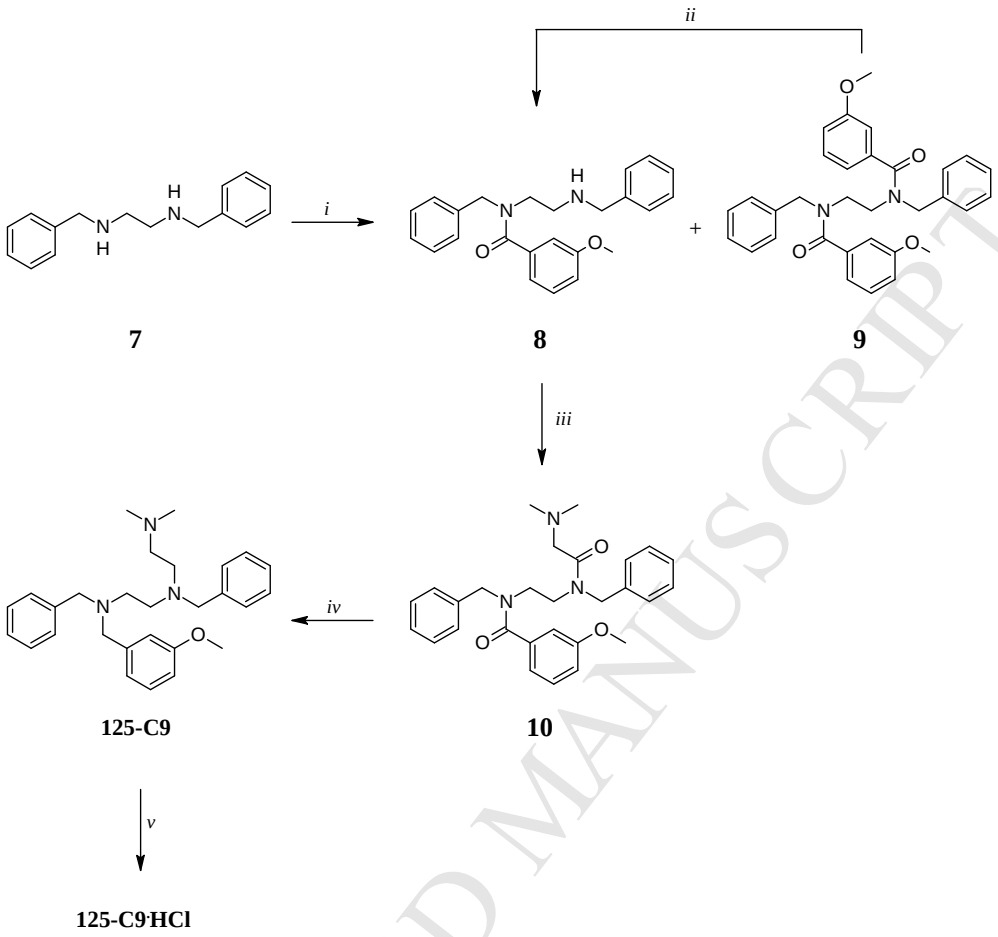

Scheme 2. *Reagents and conditions*: (i) 3-methoxybenzoyl chloride, DBU, anhyd CH_2Cl_2, 0 °C, 2 h; (ii) 12 M HCl, THF, MW, 120 °C, 20 min; (iii) *N*,*N*-dimethylglycine, EEDQ, $CHCl_3$, MW, 100 °C, 15 min; (iv) $LiAlH_4$, anhyd THF, reflux, 20 h; (v) Et_2O, gaseous HCl.

2.3. Molecular modelling: binding site mapping and docking of lubeluzole to CaM

The accessibility of CaM molecular surface was envisaged through a proper investigation carried out in order to characterize the multiple binding clefts of this biological target. It is indeed true that CaM binds diverse agonists with different stechiometry, as proved by X-ray data of more than one CaM-trifluoperazine complex [10,43,44]. To achieve this topic FPOCKET (ver 2.0) [45], a protein pocket prediction algorithm based on Voronoi tessellation was selected as a tool for our binding pocket characterization and ranking. Beside a simple visualization, that

might be at glance the first interpretation of a protein binding surface, FPOCKET also scores the detected clefts with some straight parameters (i.e. extension, hydrophobicity, polarity, and charge) which might be useful for a deeper understanding of the chemical and geometrical *cliche* of a molecular target.

In our study four main clefts, with quite different extension, and located between the symmetrical crevice of the α-helices bundle of CaM, were identified on the molecular surface of CaM, as it can be perceived in Fig. 4.

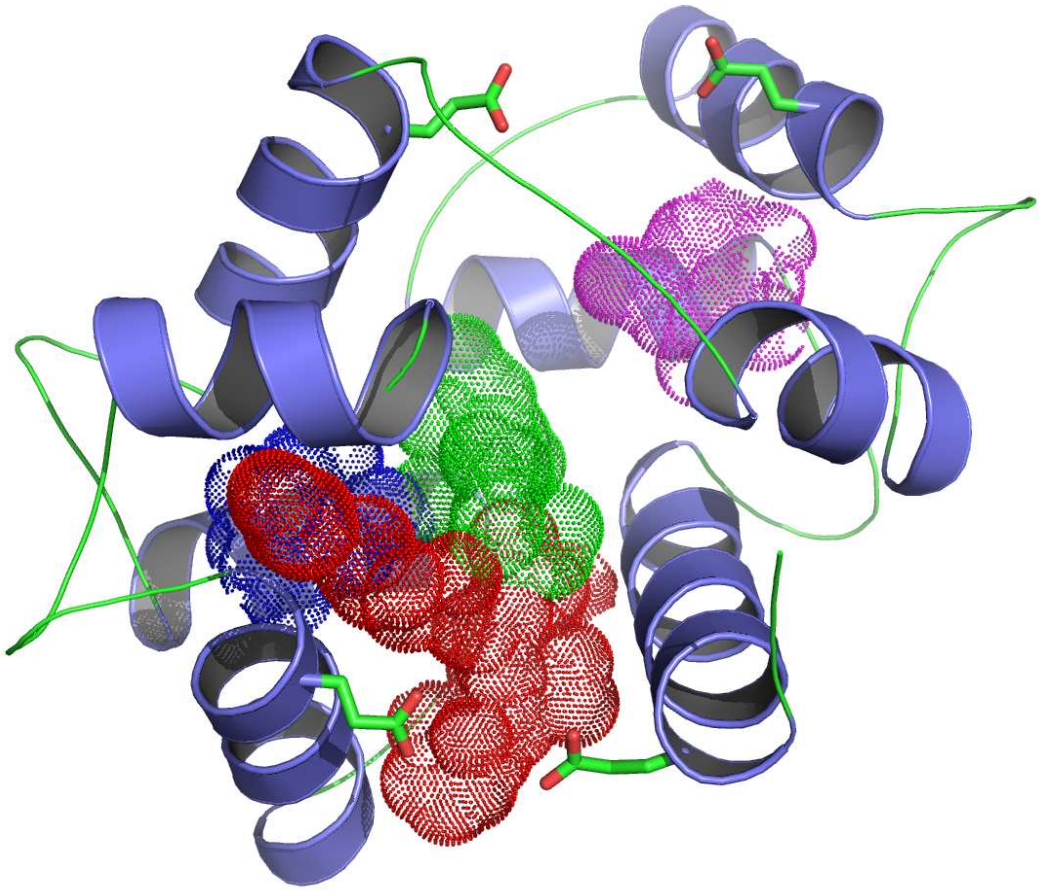

Fig.4. Binding site mapping of CaM surface as achieved by FPOCKET. The four P1, P2, P3 and P4 pockets are depicted in red, magenta, blue, and green, respectively.

In details, the **P1** cleft reveals the largest surface as well as the highest pocket score, according to the FPOCKET scoring method (Table 3). It is interesting to note that, as observed in the X-ray structure of the 1:4 complex, **P1** is completely fulfilled by a trifluoperazine molecule and also partially by the tricyclic moiety of a second trifluoperazine, suggesting that this might be the high affinity, or at least the primary, CaM ligand-binding site. As long as this evidence is concerned a secondary accessible crevice **P2**, accepting a third antagonist molecule, is located, as well as **P1**, near the two ionic pinches, comprising Glu7 and 127, and Glu54 and 84 respectively. It might be argued that these two distinct cavities might be mandatorily occupied by ligands in order to successfully hamper CaM from it elongated dumb-bell to a compact globular, and therefore inactive, conformation. To get further insights into CaM antagonism, we decided to investigate further by docking the most promising compound of our data set, lubeluzole [(*S*)-**1**], on the target structure.

Table 3
FPOCKET scoring

	P1	**P2**	**P3**	**P4**
real volume (Å^3)	1163.630	322.450	241.576	937.935
pocket score	31.144	16.342	15.730	9.731
druggability score	0.659	0.781	0.840	0.811

Due to the complexity and diversity of CaM binding surface, in a first issue we performed blind dockings as a preliminary step useful for the identification of a suitable, and eventually multiple, binding mode. Overall the three-dimensional structure of CaM-trifluoperazine complex shows a globular-shaped protein with a large and central cavity, most likely occupied by

antagonists. Two domains are arranged symmetrically so that hydrophobic surfaces lie opposite each other forming a tunnel, with acidic residues of the α-helices from both domains lying outside the same tunnel in negatively-charged patches [44]. This entire conformational space was therefore sampled by means of AUTODOCK (ver. 4.2) [46].

Because of both extended target area and considerable ligand flexibility, it was impossible to retrieve cluster poses with a valuable number of members, so as selection criterion for the supposed binding mode we chose the one endowing the best free energy of binding (FEB) to carried out further and more refined dockings (see Methods section) arising a plausible binding mode for lubeluzole [(*S*)-**1**]. The best FEB pose placed lubeluzole [(*S*)-**1]** into the largest and highest pocket score **P1** pocket**,** but nonetheless the same ligand might explore alternative binding most likely referred to **P2** pocket.

In particular, while an intramolecular hydrogen bond redirects the difluorophenoxy rings towards one EF domain, the benzothiazole fragment is deeply buried in a highly hydrophobic moiety, having its aromatic ring patched through an *edge-to-face* π-π stacking to the side chain of Phe92, and arising other favorable Van der Waals with Leu105, Met109, Met124 (see Fig. 5). The basic centre is anchored to the carboxy group of Glu127 while the hydroxyl groups stabilizes the complex making a charged reinforced hydrogen bond to negatively charged head of Glu7. This same evidence is not achieved in the binding of lubeluzole [(*S*)-**1**] to **P2**, which might therefore correspond to a secondary, or at least less relevant, binding site.

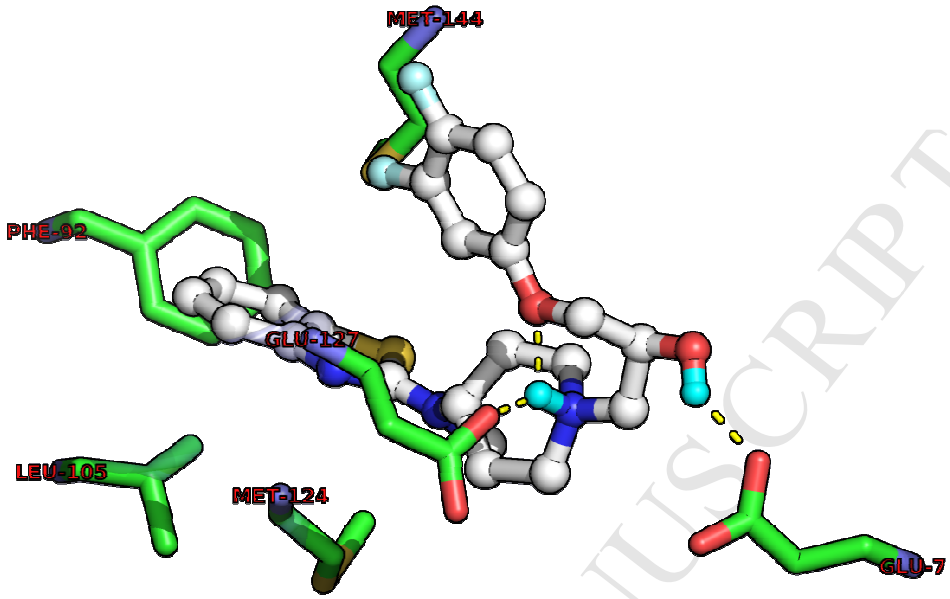

Fig.5. Binding mode of lubeluzole to CaM. Side chains of Phe92, Leu105, Met109, and Met124 are displayed to help interpretation, with C-alpha atoms being coloured in blue.

Overall this results into a free energy of binding (FEB) = –6.27 kcal/mol, corresponding to an estimated pK_i = 4.60 quite similar to the experimental pK_d value. It's interesting to note that the chair binding conformation of the piperidine ring reproduces quite well the X-ray structure [47], so there should be no interconversion phenomenon of the aliphatic cycle in the binding site.

It has been shown that the two hydrophobic binding pockets of *C*- and *N*-terminal domains, formed only when Ca^{2+} ions are bound to CaM, are the key recognition sites for both inhibitors and target enzymes [44], included Ca^{2+}/calmodulin-dependent kinase II (CaMKII) [48]. This evidence could explain the antagonist behaviour of lubeluzole on CaMKII.

3. Conclusions

A FTPFACE method was developed and validated by application to reference set of potent CaM ligands, among which the potent antagonist 125-C9 was *ad hoc* synthesized through an improved synthetic procedure. The affinity values obtained for most of the studied compounds (Table S1) were in agreement with those reported in the literature. These results demonstrate that the method proposed might be used for routine affinity analyses to individuate potent CaM ligands. The major advantages of this method are its efficiency, the possibility of testing both CaM and ligands without labelling them, and finally the possibility of testing ligands without previous separation from excipients. The method herein described was successful in disclosing a new potent CaM ligand—lubeluzole. It was slightly less potent than 125-C9 (K_d = 2.9 ± 0.7 and 0.47 ± 0.06 μM, respectively) and performed as a Ca^{2+}/calmodulin-dependent kinase II (CaMKII) inhibitor too. Docking studies based on the X-ray crystal structures of several trifluoperazine-CaM complexes have been performed in order to explore possible binding modes of lubeluzole to CaM and the main aminoacidic residues and interactions contributing to complex formation were highlighted. An estimated dissociation constant in good agreement with the experimental one was found. Thus, the ability of lubeluzole to antagonize CaM activities might contribute to its observed chemosensitizing properties. However, given the difference observed between potencies displayed in the above and the previously reported activities, further investigations are required in order to achieve new insights into the complex mechanism behind lubeluzole chemosensitizing action.

4. Experimental section

4.1. Capillary electrophoresis

4.1.1. Apparatus

Capillary electrophoresis experiments were performed using a P/ACE MDQ Beckman instrument (Palo Alto, CA, USA), equipped with a diode-array spectrophotometric detector. The fused-silica capillary was 60 cm length (50 cm to the detector) and 50 μm i.d., and was purchased from Quadrex corporation (Woodbridge, CT, U.S.A). The temperature of the capillary was 25 °C. The samples were injected by pressure: 5 psi for 30 s for CaM, followed by 0.5 psi for 5 s for ligands. The applied voltage was 20 kV. Before each run, the capillary was conditioned for 3 min with 0.1 M NaOH, for 3 min with H_2O, and for 5 min with the run buffer. Detection was performed at 220 nm.

4.1.2. Chemicals

Bovine brain CaM was purchased from Calbiochem (Merck KGaA, Darmstadt, Germany), W-7 hydrochloride [*N*-(6-aminohexyl)-5-chloronaphthalene-1-sulfonamide], clozapine [8-chloro-11-(4-methyl-1-piperazinyl)-5H-dibenzo[b,e][1,4]-diazepine], promethazine hydrochloride [10-[2-(dimethylamino)propyl]phenothiazine hydrochloride], trifluoperazine dihydrochloride [10-[3-(4-methylpiperazin-1-yl)propyl]-2-(trifluoromethyl)-10*H*-phenothiazine dihydrochloride], tris(hydroxymethyl)aminomethane (Tris), glycine, and HPLC grade ethanol were from Sigma-Aldrich (Milwaukee, WI, USA); 0.1 M sodium hydroxide was from J. T. Baker (Deventer, The Netherlands); sodium hydrogen phosphate, sodium dihydrogen phosphate, sodium borate, and deionized water (conductivity ≤0.1 μS/cm) were from Carlo Erba (Milan, Italy). Loperamide hydrochloride [4-(*p*-chlorophenyl)-4-hydroxy-*N*,*N*-dimethyl-α,α-diphenyl-1-piperidinebutyramide hydrochloride] (Imodium® gelcaps) was from Johnson & Johnson S.p.a., chlorpromazine hydrochloride [3-(2-chloro-10*H*-phenothiazin-10-yl)-*N*,*N*-dimethyl-propan-1-

amine hydrochloride] (Prozin®, oral drops) was from Lusofarmaco S.p.a., fendiline hydrochloride [*N*-(3,3-diphenylpropyl)-α-methylbenzylamine hydrochloride] and prenylamine hydrochloride [*N*-(1-methyl-2-phenylethyl)-3,3-diphenylpropan-1-amine hydrochloride] were synthesized in house by reduction of the product obtained condensating 3,3-diphenylpropionic acid (Sigma-Aldrich) and 1-phenylethylamine (Sigma-Aldrich) or between 3,3-diphenylpropionic acid (Sigma-Aldrich) and 1-methyl-2-phenylethylamine, respectively.

4.1.3. Preparation of samples and buffer

All the aqueous solutions were prepared by using deionized water. The buffer used for ACE experiments was prepared by adding a 380 mM glycine solution to 50 mM Tris until pH 8.35 was reached. In the resultant solution, $CaCl_2$ was added to reach 3 mM concentration. This buffer was used to prepare a 10 mg/ml (600 μM) stock solution of CaM, and later to opportunely dilute it to 1–0.025 mg/ml (60–1.25 μM). 10 mg/ml stock solutions of the ligands and the neutral marker (mesityl oxide) were prepared in absolute ethanol. For testing loperamide CaM affinity, the content of one Imodium® gelcap containing 2 mg of loperamide was taken up with 200 μL of absolute ethanol; this mixture was sonicated for 20 min and then filtered. In the case of chlorpromazine, the 40 mg/ml solution of Prozin® was diluted 1:4 with absolute ethanol. Afterwards the sample stock solutions were diluted 1:100 with water.

Phosphate and borate buffers for pK_a determinations were prepared by combining appropriate amounts of 0.033 M Na_2HPO_4 and 0.033 M NaH_2PO_4 solutions, or 0.025 M $Na_2B_4O_7$ and 0.025 NaOH solutions to achieve the proper pH in the range 6.80–9.80.

All the solutions were filtered through a PTFE mesh 0.20 μM porous size (Advantec MFS, Dublin, CA, USA) and stored at 4 °C until usage.

4.2. Chemistry

All chemicals were purchased from Sigma–Aldrich or Lancaster at the highest quality commercially available. Solvents were RP grade unless otherwise indicated. Yields refer to purified products and were not optimized. The structures of the compounds were confirmed by routine spectrometric and spectroscopic analyses. Only spectra for compounds not previously described are given. Melting points were determined on a Gallenkamp apparatus in open glass capillary tubes and are uncorrected. Infrared spectra were recorded on a Perkin–Elmer (Norwalk, CT) Spectrum One FT spectrophotometer and band positions are given in reciprocal centimeters (cm^{-1}). ^{1}H and ^{13}C NMR spectra were recorded on a Varian Mercury-VX spectrometer (Varian Inc., Palo Alto, CA, USA), operating at 300 and 75 MHz for ^{1}H and ^{13}C, respectively, or on a Agilent Technologies 500 MHz (Varian Inc., Palo Alto, CA, USA), operating at 500 and 126 MHz for ^{1}H and ^{13}C, respectively, using $CDCl_3$ as solvent, unless otherwise indicated. Chemical shifts are reported in parts per million (ppm) relative to solvent resonance: $CDCl_3$, δ 7.26 (^{1}H NMR) and δ 77.3 (^{13}C NMR). *J* values are given in Hz. EIMS spectra were recorded on a Hewlett-Packard 6890-5973 MSD gas chromatograph/mass spectrometer (Hewlett-Packard, Palo Alto, CA, USA) at low resolution. $ESI^{+/-}$/MS/MS analyses were performed with an Agilent 1100 series LC-MSD trap system VL Workstation (Agilent, Palo Alto, CA, USA). Elemental analyses were performed with a Eurovector Euro EA 3000 analyzer. Chromatographic separations were performed on silica gel columns by flash chromatography (Kieselgel 60, 0.040–0.063 mm, Merck, Darmstadt, Germany). TLC analyses were performed on precoated silica gel on aluminum sheets (Kieselgel 60 F254, Merck).

*4.2.1. Acylation of N,N'-dibenzylethylenediamine (**8**)*

To an ice-cold solution of *N*,*N*'-dibenzylethylenediamine (**7**, 2.0 g, 8.33 mmol) and DBU (0.89 g, 5.86 mmol) in dry CH_2Cl_2 (30 mL), a solution of 3-methoxybenzoyl chloride (0.71 g, 4.18 mmol) in dry CH_2Cl_2 (15 mL) was added dropwise under N_2 atmosphere. The reaction mixture was stirred at 0 °C for 90 min and then the solid was filtered off. The filtrate was diluted with CH_2Cl_2 (40 mL) and washed twice with 2 M NaOH (40 mL) and twice with brine (20 mL). The organic phase was dried (anhydrous Na_2SO_4) and concentrated under vacuum. The residue was purified by flash chromatography (EtOAc) to give **8** and **9**.

*4.2.1.1. N-benzyl-N-[2-(benzylamino)ethyl]-3-methoxybenzamide (**8**)*

Yellowish oil (0.79 g, 51%); IR (neat): 3317 (NH), 1630 (C=O) cm^{-1}; ^{1}H NMR (300 MHz): δ 1.48 (br s, 1H, exch D_2O), 2.90 (br s, 2H), 3.32 (br s, 2H), 3.59 (br s, 2H), 3.72 (br s, 3H), 4.56 (br s, 2H), 6.92 (br d, *J* = 8.5 Hz, 1H), 6.95 (br s, 1H), 6.99 (dd, *J* = 7.4, 1.1 Hz, 1H), 7.10–7.21 (m, 1H), 7.22–7.40 (m, 10H); ^{13}C NMR (500 MHz): δ 44.8 (1C), 46.7 (1C), 48.2 (1C), 53.6 (1C), 55.2 (1C), 112.0 (1C), 115.6 (1C), 118.8 (1C), 127.0 (1C), 128.0 (1C), 128.4 (4C), 128.8 (4C), 129.6 (1C), 137.7 (2C), 140.2 (1C), 159.6 (1C), 172.2 (1C); ESI$^+$/MS *m/z*: 397 [M + Na^+]; ESI$^+$/MS/MS *m/z*: 268 (100).

*4.2.1.2. N,N'-1,2-ethanediylbis[N-(phenylmethyl)-3-methoxybenzamide] (**9**)*

White solid (0.36 g, 33%); mp: 130–131 °C; IR (KBr): 1631 (C=O) cm^{-1}; ^{1}H NMR (300 MHz): δ 3.65 (s, 6H), 3.76 (s, 4H), 4.72 (s, 4H), 6.89 (d, *J* = 8.1 Hz, 2H), 6.99 (s, 2H), 7.04 (d, *J* = 7.2 Hz, 2H), 7.19 (apparent t, 2H), 7.22–7.50 (m, 10H); ^{1}H NMR (toluene-d_8, 500 MHz): δ 3.25 (s, 6H), 3.58 (s, 4H), 4.69 (s, 4H), 6.70 (d, *J* = 6.4 Hz, 2H), 6.90–7.15 (m, 14H), 7.24 (s, 2H); ^{13}C

NMR (300 MHz): δ 40.7 (2C), 52.5 (2C), 55.4 (2C), 111.9 (2C), 116.2 (2C), 119.1 (2C), 127.4 (2C), 127.9 (2C), 129.0 (6C), 129.9 (2C), 137.0 (2C), 137.6 (2C), 159.8 (2C), 172.6 (2C); ESI^+/MS *m/z*: 531 [M + Na^+]; ESI^+/MS/MS *m/z*: 268 (100); Anal. Calcd for ($C_{32}H_{32}N_2O_4 \cdot 0.33H_2O$): C, 74.69; H, 6.40; N, 5.44. Found: C, 74.86; H, 6.32; N, 5.52.

*4.2.2. Hydrolysis of **9***

A solution of **9 (**0.23 g, 0.45 mmol) in THF (4 mL) and 12 N HCl (10 mL) was stirred for 20 min at 120 °C in a microwave reactor. When the reaction was completed, the mixture was cooled and NaOH pellets were added. The aqueous phase was extracted three times with EtOAc and the combined organic phases were dried (anhydrous Na_2SO_4) and concentrated under reduced pressure. Purification of the residue by flash chromatography (EtOAc/petroleum ether 1:1, then MeOH/EtOAc 1:9) gave 0.10 g (62%) of **8**.

*4.2.3. N-benzyl-N-{2-[benzyl(N,N-dimethylglycyl)amino]ethyl}-3-methoxybenzamide (**10**)*

A solution of **8 (**0.30 g, 0.80 mmol), *N*,*N*-dimethylglycine hydrochloride (0.11 g, 0.80 mmol) and EEDQ (0.24 g, 0.96 mmol) in $CHCl_3$ (20 mL) was stirred for 15 min at 100 °C in a microwave reactor. After evaporation of the solvent, the residue was taken up with EtOAc, washed with 2 N NaOH, and then with brine. The organic phase was dried over anhydrous Na_2SO_4 and concentrated under reduced pressure. The residue was purified by flash chromatography (EtOAc/petroleum ether 9:1, then EtOAc) to give 0.24 g (65%) of **10** as a yellow oil: IR (neat): 1635 (C=O) cm^{-1}; ^1H NMR (toluene-d_8, 500 MHz): δ 2.10 (s overlapping solvent resonance, 6H), 2.18 (s, 2H), 3.22 (s, 2H), 3.33 (s, 3H), 3.56 (s, 2H), 4.60 (s, 2H), 4.76 (s, 2H), 6.73 (br d, *J* = 7.3 Hz, 1H), 6.86 (br s, 1H), 6.94–7.20 (m, 11H), 7.31 (br s, 1H); ^{13}C NMR (500 MHz): δ 41.3

(1C), 42.0 (1C), 45.7 (2C), 50.3 (1C), 52.6 (1C), 55.2 (1C), 61.8 (1C), 111.9 (1C), 115.8 (1C), 118.8 (1C), 126.7 (1C), 127.1 (1C), 128.6 (4C), 128.9 (4C), 129.7 (1C), 136.9 (2C), 137.3 (1C), 159.6 (1C), 170.9 (1C), 172.2 (1C); ESI^+/MS *m/z*: 482 [M + Na^+]; ESI^+/MS/MS *m/z*: 482 (100).

4.2.4. N,N'-dibenzyl-N-[2-(dimethylamino)ethyl]-N'-(3-methoxybenzyl)ethane-1,2-diamine (125-C9)

To a stirred solution of **10** (0.24 g, 0.52 mmol) in dry THF (15 mL), $LiAlH_4$ (0.20 g, 5.2 mmol) was added under N_2 atmosphere. The reaction mixture was heated at reflux for 20 h, then it was cooled with an ice bath and quenched by the careful addition of cold water until the end of gas evolution. The residue was removed by filtration and the filtrate additioned with water. The aqueous phase was acidified with 2 M HCl, washed with EtOAc, then made alkaline with NaOH pellets and extracted with EtOAc. The combined organic phases were dried (anhydrous Na_2SO_4) and concentrated under reduced pressure to afford 125-C9 (0.20 g, 89%) as light-brown oil: ^{1}H NMR (500 MHz): δ 2.13 (s, 6H), 2.31 (dd, *J* = 8.6, 6.1 Hz, 2H), 2.49 (dd, *J* = 8.6, 6.1 Hz, 2H), 2.54–2.60 (m, 2H), 2.61–2.67 (m, 2H), 3.54 (s, 4H), 3.55 (s, 2H), 3.78 (s, 3H), 6.76 (dd, *J* = 7.6, 2.2 Hz, 1H), 6.91 (d, *J* = 7.8 Hz, 1H), 6.93 (s, 1H), 7.18–7.34 (m, 10H), 7.37 (br d, *J* = 5.4 Hz, 1H); ^{13}C NMR (500 MHz): δ 45.8 (2C), 51.2 (1C), 52.2 (1C), 52.3 (1C), 55.1 (1C), 57.6 (1C), 58.79 (1C), 58.83 (1C), 59.4 (1C), 112.2 (1C), 114.1 (1C), 121.0 (1C), 126.76 (1C), 126.79 (1C), 128.10 (2C), 128.14 (2C), 128.7 (2C), 128.8 (2C), 129.1 (1C), 139.5 (1C), 139.7 (1C), 141.6 (1C), 159.6 (1C); MS (70 eV) m/z (%) 373 (M^+ – 58, 42), 91 (100).

4.2.5. N,N'-dibenzyl-N-[2-(dimethylamino)ethyl]-N'-(3-methoxybenzyl)ethane-1,2-diamine hydrochloride (125-C9·3HCl)

125-C9 (0.20 g, 0.46 mmol) was dissolved in dry Et_2O and treated with gaseous HCl for a few seconds to give a white solid, which was recrystallized from abs EtOH/Et_2O to afford 0.11 g of white crystals (44%): mp 190–192 °C; ^{1}H NMR (CD_3OD, 500 MHz): δ 2.87 (s, 6H), 3.48 (br s, 2H), 3.50–3.70 (m, 6H), 3.83 (s, 3H), 4.16 (br s, 2H), 4.38 (s, 2H), 4.43 (s, 2H), 7.02 (dd, *J* = 8.3, 2.4 Hz, 1H), 7.12 (d, *J* = 7.3 Hz, 1H), 7.24 (s, 1H), 7.36 (apparent t, 1H), 7.40–7.64 (m, 10H); ^{13}C NMR (500 MHz): δ 42.5 (2C), 48.2 (2C), 54.7 (2C), 57.8 (3C), 58.0 (1C), 116.0 (1C), 116.3 (1C), 123.2 (1C), 128.7 (1C), 128.9 (1C), 129.08 (1C), 129.14 (4C), 130.1 (1C), 130.2 (1C), 130.8 (1C), 131.4 (4C), 160.4 (1C); ESI$^+$/MS *m/z*: 432 [M + H$^+$]; ESI$^+$/MS/MS *m/z*: 205 (100); Anal. Calcd for ($C_{28}H_{37}N_3O$·3HCl·H_2O): C, 60.16; H, 7.57; N, 7.52. Found: C, 60.50; H, 7.47; N, 7.77.

4.3. CaMKII activity assay

CaMKII activity was tested on Autocamtide in the presence of the tested compounds. In a first reaction step, active recombinant full-length CaMKII (Signal Chem, La Jolla) was incubated for 30 min at 30 °C with 1 mmol/L $CaCl_2$ and 5 μmol/L CaM in 50 μL of a reaction mixture (50 mmol/L HEPES pH 7.5, 10 mmol/L $MgCl_2$, 0.5 mmol/L dithiothreitol (DTT), 100 nmol/L microcystin, 0.1 mmol/L non-radiolabeled ATP) [49]. In a second reaction step, a 10 μL aliquot from the first reaction was then incubated with 25 mM EGTA, 0.2 μCi/μl of Easy Tides Adenosine 5'-triphosphate [γ^{32}P]-ATP (Perkin Elmer) and 0.5 mM Autocamtide [50] in the presence of the tested compounds (at different concentrations) in order to determine the effects

of the compounds on CaMKII activity on its substrate Autocamtide. AntCaNtide at a concentration of 5 μM was used as positive control of CaMKII inhibition. The reaction was carried out for 30 min at 30 °C, then 20 μL aliquots of the reaction mixture were spotted onto Whatman P-81 phosphocellulose paper. EGTA was added to quantify CaMKII autonomous activity. Dried filters were counted on a Beckman LS 6000 scintillation counter.

4.4. Molecular modeling

The 2.0 Å resolution Ca^{2+}/CaM-trifluoperazine 1:4 complex X-ray structure (entry code 1LIN) was taken from the Protein Data Bank and passed to the Protein Preparation Wizard implemented in the MAESTRO software package [MacroModel, version 9.9, Schrödinger, LLC, New York, NY, 2012]. The complex was stripped out of solvent and ligands and all the hydrogens were added and their positions refined; the point charges for each atom were calculated according to AMBER force field [51]. As a result, protein affinity maps were calculated with AUTOGRID as follow: in the first blind docking a 80×80×80 0.5 Å spaced cubic box was built around the center of mass of the protein, while for the refinement dockings a more spaced (0.375 Å) cage was indeed considered.

The lubeluzole X-ray (CSD code) was downloaded from the Cambridge Structural Database and submitted to the energy minimization and electrostatic charges calculation according to the quanto-mechanical method AM1 implemented in MAESTRO. The indirect method to manage the ring as a fully flexible entity during the AUTODOCK conformation search was applied [52]. This protocol converts the cyclic ligand into its corresponding acyclic form by removing a bond.

Bonds between two identical atom types (C-C) and resulting in shorter chains were preferred to keep the calculation simple and improve the quality of the final results.

Due to the conformational freedom of the ligand, the maximum number of energy evaluations was set to 25 millions. Lamarckian genetic algorithm (LGA) was carried out for 100 and 500 runs during the blind and refinement docking respectively. In the first 100 runs the tran0, quat0 and dihe0 were set to random, while in the latest 500 runs the same values were set to the values suggested by the same LGA for the best FEB pose.

Acknowledgments

The authors thank the Ministero dell'Istruzione, dell'Università e della Ricerca (MIUR) (Project PRIN 2010FPTBSH_005 "NANO Molecular tEchnologies for Drug delivery – NANOMED") for financial help. The authors are indebted to dr. Ottavio Ungaro for his invaluable help.

References

[1] M. De Ryck, R. Keersmaekers, H. Duytschaever, C. Claes, G. Clincke, M. Janssen, G. Van Reet, J. Pharmacol. Exp. Ther. 279 (1996) 748–758.

[2] A.S. Lesage, L. Peeters, J.E. Leysen, J. Pharmacol. Exp. Ther. 279 (1996) 759–766.

[3] D. Scheller, J. Kolb, S. Szathmary, E. Zacharias, M. De Ryck, J. Van Reempts, G. Clincke, F. Tegtmeier, J. Cereb. Blood Flow Metab. 15 (1995) S379.

[4] R.N. Mueller, D.J. Deyo, D.R. Brantley, J.F. Disterhoft, M.H. Zornow, Exp. Brain Res. 152 (2003) 329–334.

[5] M.M. Cavalluzzi, M. Viale, C. Bruno, A. Carocci, A. Catalano, A. Carrieri, C. Franchini, G. Lentini, Bioorg Med Chem Lett 23 (2013) 4820–4823.

[6] J.-F. Desaphy, R. Carbonara, T. Costanza, G. Lentini, M.M. Cavalluzzi, C. Bruno, C. Franchini, D. Conte Camerino, Mol. Pharmacol. 83 (2013) 406–415.

[7] G.C. Davis, Y. Kong, M. Paige, Z. Li, E.C. Merrick, T. Hansen, S. Suy, K. Wang, S. Dakshanamurthy, A. Cordova, O.B. McManus, B.S. Williams, M. Chruszcz, W. Minor, M. K. Patel, M.L. Brown, Bioorg. Med. Chem. 20 (2012) 2180–2188.

[8] A. Arcangeli, O. Crociani, E. Lastraioli, A. Masi, S. Pillozzi, A. Becchetti, Curr. Med. Chem. 16 (2009) 66–93.

[9] H.C. Diener, W. Hacke, M. Hennerici, J. Rådberg, L. Hantson, J. De Keyser, Stroke 27 (1996) 76–81.

[10] P. James, T. Vorherr, E. Carafoli, Trends Biochem. Sci. 20 (1995) 38–42.

[11] B.G. Vertessy, V. Harmat, Z. Böcskei, G. Náray-Szabó, F. Orosz, J. Ovádi, Biochemistry 37 (1998) 15300–15310.

[12] E. Teodori, S. Dei, S. Scapecchi, F. Gualtieri, Farmaco 57 (2002) 385–415.

[13] Y.C. Mayur, S. Jagadeesh, K. N. Thimmaiah, Mini-Rev. Med. Chem. 6 (2006) 1383–1389.

[14] R. Liu, Y. Zhang, Y. Chen, J. Qi, S. Ren, M.Y. Xushi, C. Yang, H. Zhu, D. Xiong, J. Pharm. Sci. 99 (2010) 3266–3275.

[15] J. Colomer, A.A. Schmitt, E.J. Toone, A.R. Means, Biochemistry 49 (2010) 4244–4254.

[16] P.G. Daft, K. Yuan, J.M. Warram, M.J. Kein, G.P. Siegal, M. Zayzafoon, Mol. Cancer Res. 11 (2013) 349–359.

[17] C. Riganti, S. Doublier, D. Viarisio, E. Miraglia, G. Pescarmona, D. Ghigo, A. Bosia, Br. J. Pharmacol. 156 (2009) 1054–1066.

[18] O.A. Mamaeva, J. Kim, G. Feng, J.M. McDonald, J.Cell. Biochem. 106 (2009) 25–32.

[19] S. Hishinuma, K. Ogura, J. Neurochem. 75 (2000) 772–781.

[20] J.S. Shim, J. Lee, K.N. Kim, H.J. Kwon, Biochem. Biophys. Res. Commun. 359 (2007) 747–751.

[21] A.G. Turjanski, D.A. Estrin, R.E. Rosenstein, J.E. McCormick, S.R. Martin, A. Pastore, R.R. Biekofsky, V. Martorana, Protein Sci. 13 (2004) 2925–2938.

[22] V. Harmat, Z. Böcskei, G. Náray-Szabó, I. Bata, A.S. Csutor, I. Hermecz, P. Arányi, B. Szabó, K. Liliom, B.G. Vértessy, J. Ovádi, J. Mol. Biol. 297 (2000) 747–755.

[23] P. Nokin, J.P. Blondiaux, P. Schaeffer, L. Jungbluth, C. Lugnier, Naunyn-Schmiedeberg's Arch. Pharmacol. 339 (1989) 367–373.

[24] H. Ouyang, H.J. Vogel, Biochim. Biophys. Acta 1383 (1998) 37–47.

[25] M. González-Andrade, J. Rivera-Chávez, A. Sosa-Peinado, M. Figueroa, R. Rodríguez-Sotres, R. Mata, J. Med. Chem. 54 (2011) 3875–3884.

[26] I. Fitos, J. Visy, J. Kardos, M. Simonyi, Chirality 7 (1995) 69–73.

[27] H. Itoh, T. Tanaka, Y. Mitani, H. Hidaka, Biochem. Pharmacol. 35 (1986) 217–220.

[28] P.F. Morgan, J. Patel, P.J. Marangos, Biochem. Pharmacol. 36 (1987) 4257–4262.

[29] F. Friedberg, A.R. Rhoads, IUBMB Life 51 (2001) 215–221.

[30] Y.H. Chu, L.Z. Avila, H.A. Biebuyck, G.M. Whitesides, J. Med. Chem. 35 (1992) 2915–2917.

[31] R. Schreiber, J. Membrane Biol. 205 (2005) 129–137.

[32] P. Vaupel, F. Kallinowski, P. Okunieff, Cancer Res. 49 (1989) 6449–6465.

[33] L. Li, C. Li, Z. Zhang, E. Alexov, J. Chem. Theory Comput. 9 (2013) 2126–2136.

[34] D.K. Menyhárd, G.M. Keserű, G. Náray-Szabó, Curr. Comput.-Aided Drug Des. 5 (2009) 264–279.

[35] I. Kövesi, D.K. Menyhárd, M. Laberge, J. Fidy, J. Med. Chem. 51 (2008) 3081–3093.

[36] J.-F. Zhang, L. Ma, X. Liu, Y.-T. Lu, J. Chromatogr. B Analyt. Technol. Biomed. Life Sci. 804 (2004) 413–420.

[37] H. Kajiwara, H. Hirano, K. Oono, J. Biochem. Biophys. Methods 22 (1991) 263–268.

[38] J. Heintz, M. Hernandez, F.A. Gomez, J. Chromatogr. A 840 (1999) 261–268.

[39] A. Carocci, A. Catalano, C. Bruno, A. Lovece, M.G. Roselli, M.M. Cavalluzzi, F. De Santis, A. De Palma, M.R. Rusciano, M. Illario, C. Franchini, G. Lentini, Bioorg. Med. Chem. 21 (2013) 847–851.

[40] D.S. Shapenova, M.K. Belyatskii, L.P. Panicheva, Russ. J. Org. Chem. 46 (2010) 1017–1020.

[41] C. Bruno, A. Carocci, A. Catalano, M.M. Cavalluzzi, F. Corbo, C. Franchini, G. Lentini, V. Tortorella, Chirality 18 (2006) 227–231.

[42] M. Singh, U.C. Banerjee, Tetrahedron: Asymmetry, 18 (2007) 2079–2085.

[43] W.J. Cook, L.J. Walter, M.R. Walter, Biochemistry 33 (1994) 15259–15265.

[44] M. Vandonselaar, R.A. Hickie, J.W. Quail, L.T. Delbaere, Nat. Struct. Biol. 1 (1994) 795–801.

[45] V. Le Guilloux, P. Schmidtke, P. Tuffery, BMC Bioinformatics 10 (2009):168. doi:10.1186/1471-2105-10-168

[46] G.M. Morris, R. Huey, W. Lindstrom, M.F. Sanner, R.K. Belew, D.S. Goodsell, A.J. Olson, J. Comput. Chem. 16 (2009) 2785–2791.

[47] O.M. Peeters, N.M. Blaton, C.J. De Ranter, Acta Crystallogr., Sect. C: Cryst. Struct. Commun. C51 (1995) 2129–2132.

[48] S.S. Hook, A.R. Means, Annu. Rev. Pharmacool. Toxicol. 41 (2001) 471–505.

[49] D. Chin, K.E. Winkler, A.R. Means, J. Biol. Chem. 272 (1997) 31235–31240.

[50] P.I. Hanson, M.S. Kapiloff, L.L. Lou, M.G. Rosenfeld, H. Schulman, Neuron 3 (1989) 59–70.

[51] W.D. Cornell, P. Cieplak, C.I. Bayly, I.R. Gould, K.M. Merz, D.M. Ferguson, D.C. Spellmeyer, T. Fox, J.W. Caldwell, P.A. Kollman, J. Am. Chem. Soc. 117 (1995) 5179–5197.

[52] S. Forli, M. Botta, J. Chem. Inf. Model. 47 (2007) 1481–1492.

[53] J.D. Johnson, L.A. Wittenauer, Biochem. J. 211 (1983) 473–479.

[54] J.H. Zavecz, T.E. Jackson, G.L. Limp, T.O. Yellin, Eur. J. Pharmacol. 78 (1982) 375–377.

[55] R.M. Levin, B. Weiss, J. Pharmacol. Exp. Ther. 208 (1979) 454–459.

[56] C. Nicolas, C. Carter, J. Neurochem. 63 (1994) 2248–2258.

[57] K.E. Fladmark, O.T. Brustugun, G. Mellgren, C. Krakstad, R. Bøe, O.K. Vintermyr, H. Schulman, S.O. Døskeland, J. Biol. Chem. 277 (2002) 2804–2811.

Lubeluzole affinity for CaM was evaluated through an ACE method.

The potent CaM ligand 125-C9 was synthesized through an improved synthetic procedure.

CaMKII inhibitory effect of lubeluzole was demonstrated.

Possible binding modes of lubeluzole to CaM were explored by docking studies.